Journal of Advanced Concrete Technology
Materials, Structures and Environment

Effect of Wollastonite Microfiber on Ultra-High-Performance Fiber-Reinforced Cement-Based Composites based on Application of Multi-scale Fiber-Reinforcement System

Sukmin Kwon, Tomoya Nishiwaki, Heesup Choi, Hirozo Mihashi

Journal of Advanced Concrete Technology, volume 13 (2015), pp. 332-344

Related Papers Click to Download full PDF!

Corrosion of reinforcing steel in fiber reinforced cementitious composites
Hirozo Mihashi, Shaikh Faiz Ahmed, Ayuko Kobayakawa
Journal of Advanced Concrete Technology, volume 9 (2011), pp. 159-167

Experimental Study on Self-Healing Capability of FRCC Using Different Types of Synthetic Fibers
Tomoya Nishiwaki, Marina Koda, Hirozo Mihashi, Takatsune Kikuta
Journal of Advanced Concrete Technology, volume 10 (2012), pp. 195-206

Fixed-Angle Smeared-Truss Approach with Direct Tension Force Transfer Model for Torsional Behavior of Steel Fiber-Reinforced Concrete Members
Hyunjin Ju, Deuck Hang Lee, Jin-Ha Hwang, Kang Su Kim
Journal of Advanced Concrete Technology, volume 11 (2013), pp. 215-229

Modeling of high-strength FRC members with non-uniform fiber distribution
Petr Kabele, Tereza Sajdlová, Milan Rydval, Jiří Kolisko
Journal of Advanced Concrete Technology, volume 13 (2015), pp. 311-324

Click to Submit your Papers
Japan Concrete Institute http://www.j-act.org

Scientific paper

Effect of Wollastonite Microfiber on Ultra-High-Performance Fiber-Reinforced Cement-Based Composites Based on Application of Multi-Scale Fiber-Reinforcement System

Sukmin Kwon[1*], Tomoya Nishiwaki[2] , Heesup Choi[3] and Hirozo Mihashi[4]

Received 4 August 2014, accepted 22 June 2015 doi:10.3151/jact.13.332

Abstract

The development of ultra-high-performance fiber-reinforced cement-based composites (UHP-FRCCs) was motivated by the need for a new and versatile material with high energy absorption capacity. With its excellent cracking resistance and consequent long life, UHP-FRCC is suitable for use in seismic design applications. The present study proposes a material design concept based on a multi-scale fiber-reinforcement system. In this approach, long, thick macrofibers are blended with short, thin mesofibers and microfibers. Such a combination of macrofibers, mesofibers, and microfibers is expected to enhance the mechanical properties of the composite under tension. However, the ductility of cement-based composites reinforced solely by microfibers is largely unknown. Therefore, in this study, the authors assessed whether microfiber improves the ductility of UHP-FRCC in two series of experiments. Wollastonite, which is a needle-shape mineral, is employed as a microfiber, and two different types of steel fibers are used as meso- and macrofibers. First, the enhanced toughness was evaluated in three-point bending tests on notched mortar beams. Second, the influence of wollastonite microfiber on the mechanical properties of the blended multi-scale fiber-reinforcement system was evaluated in uniaxial tension tests. Blends of macrofibers, mesofibers, and wollastonite microfibers exhibited strong reinforcement characteristics. The results indicate that the ductility of composites reinforced with wollastonite microfibers is highly dependent on the microfiber contents and type of fiber used and that blending of micro-, meso-, and macrofibers produces a highly ductile UHP-FRCC. Thus the material design concept based on the multi-scale fiber-reinforcement system proposed in this paper was shown to be effective in increasing the ductility of UHP-FRCC, even under uniaxial tension.

1. Introduction

The enhanced tensile properties of ultra-highperformance fiber-reinforced cement-based composites (UHP-FRCCs), such as tensile strength, energy absorption capacity, and toughness, have been investigated by many researchers (Magureanu *et al*. 2012). The advantages of UHP-FRCC, in comparison to ordinary concrete, include its high strength, which is to the result of its very fine microstructure and low porosity, which together are responsible for its high durability. The incorporation of fibers in the mix design for cement-based composites has been shown to increase the toughness and ductility of such composites (Ranade *et al*. 2013). The motivation for improving the mechanical properties of UHP-FRCC is the creation of a new, versatile material with a large energy absorption capacity suitable for use in seismic design applications and possessing a long service life by virtue of its crack resistance.

In the 1980s, the concept of slurry-infiltrated fiber-reinforced concrete (SIFCON) was introduced by Lankard (1984). Later, Naaman (1992) carried out the research on the improvements in the mechanical properties, including increased tensile strength and ductility, of concrete mixes containing up to 17% deformed steel fibers by volume contents. These mixes exhibited a post-cracking tensile strength of 35 MPa and a strain of 1.2% at the peak load. Bache (1992) used densified small particles (DSP) to produce mixes with compressive strengths of more than 150 MPa and used a microsilica and superplasticizer to decrease matrix porosity. By adding short, high-strength steel fibers at contents of up to 12% by volume, (Bache 1992) showed that a significant increase in the equivalent elastic bending strength, of up to 50 MPa, could be obtained and that such mixes would exhibit strain hardening behavior. However, these types of materials have high costs and poor workability due to the high fiber volume contents and are thus limited in their practical applicability.

Recently, a few notable investigations have been conducted on mixes with relatively low volume contents of fiber and relatively high strengths and strain capacities. For example, a commercial UHP-FRCC developed as part of a collaborative project between Lafarge Bouygues and Rhdia (Chanvillard and Rigaud 2003; Orange *et al*.

[1]JSPS Research Fellow, Department of Architecture and Building Science, Tohoku University, Graduate School of Engineering, Sendai, Japan.
*Corresponding author,
E-mail: sukminkwon@gmail.com
[2]Associate Professor, Department of Architecture and Building Science, Tohoku University, Graduate School of Engineering, Sendai, Japan.
[3]Assistant Professor, Department of Civil Engineering, Kitami Institute of Technology, Kitami, Japan.
[4]Professor Emeritus, Tohoku University, Sendai, Japan.

2000) exhibited a compressive strength of approximately 200 MPa, a tensile strength of 15.1 MPa, and a tensile strain of 0.3% at the peak load, achieved by incorporating 2% high-strength steel fibers by volume. In a similar collaborative study, SIKA and EIFFAGE developed a commercial UHP-FRCC (Jungwirth 2006; Maeder *et al*. 2004) with 2.5% steel fibers by volume that exhibited a compressive strength of 200 MPa, a tensile strength of 10 MPa, and a tensile strain of 0.25% at the peak load.

Taking another approach to improving the tensile properties of UHP-FRCC, Rossi *et al*. (1987) proposed multiscale cement composites (MSCC) that contained two or three different types of steel fibers, such as long or short fibers and straight or hooked fibers. However, when the steel fibers were straight but not mechanically deformed, it was not possible to obtain a strain capacity of more than 0.3%. The Laboratoire Central des Ponts et Chausses in France (LCPC) developed a commercial UHP-FRCC (Boulay *et al*. 2004) with the addition of 11% of a blend of three different steel fibers by volume that exhibited a tensile strength of 20 MPa and a tensile strain of 0.2% at the peak load.

Sujiravorakul (2002) investigated the ability of twisted high-strength fibers with exceptional bonding properties to improve the tensile properties of cement-based composites. Wille *et al*. (2011) reported the development of a UHP-FRCC with the addition of 2% twisted steel fibers by volume contents that exhibited a compressive strength of 200 MPa, a tensile strength of 14.9 MPa, and a tensile strain of 0.61% at the peak load. However, because of their special geometry, these fibers are high in cost.

Although UHP-FRCCs are high-performance materials, methods for improving their tensile properties are still not sufficiently developed. Therefore, the authors focused in this study on cracks initiated at the micro-scale, i.e., in the so-called fracture process zone, as shown in **Fig. 1**. As these cracks propagate, they progress to the meso- and macro-scales (Mihashi *et al*. 2010). In this study, the authors defined the micro-, meso- and macro-scales as being on the orders of 10^{-1} mm or less, 10^{0} mm, and 10^{1} mm or more, respectively. Furthermore, the authors proposed a method for optimizing the shape and size of fibers corresponding to various crack scales and for improving the tensile properties of cement-based composites by reinforcing from the micro- to the macro-scale.

Various types of microfibers, including metallic, organic, mineral, and synthetic microfibers, can be used as reinforcement for cement-based materials. One potential microfiber is wollastonite, which is widely used in other industrial applications (e.g., ceramics, plastics, paints). Wollastonite is a naturally produced white mineral (silicate mineral [β-CaO-SiO_2]) (Soliman and Nehdi 2012). Its fibrous structure, which is made up of needle-shaped acicular crystals, is presumed to be useful in controlling microcracks in the fracture process zone, illustrated in **Fig. 1.**

In this study, the authors assessed whether wollastonite microfibers improved the ductility of UHP-FRCC in the following two series of tests. First, the influence of various types of wollastonite microfiber at various contents on the toughness improvement of ultra-high-strength mortar (UHSM) was investigated by means of toughness index and observation on fracture surfaces of UHSM reinforced with wollastonite microfiber (Test I). Second, the reinforcement effect of wollastonite microfibers on the mechanical properties of a multi-scale fiber-reinforcement system, that is, a combination of macrofibers, mesofibers, and wollastonite microfibers (Test II).

2. Definition of toughness and ductility in this study

Toughness is defined as the ability of a material to deform plastically and to absorb energy in the process before fracture. High toughness means that cracks are hardly generated and cracks do not easily propagate in the material. Generally, toughness is used to represent the characteristic of the material with a notch or crack.

Ductility is defined as the ability of a material to withstand plastic deformation without rupture. Ductile

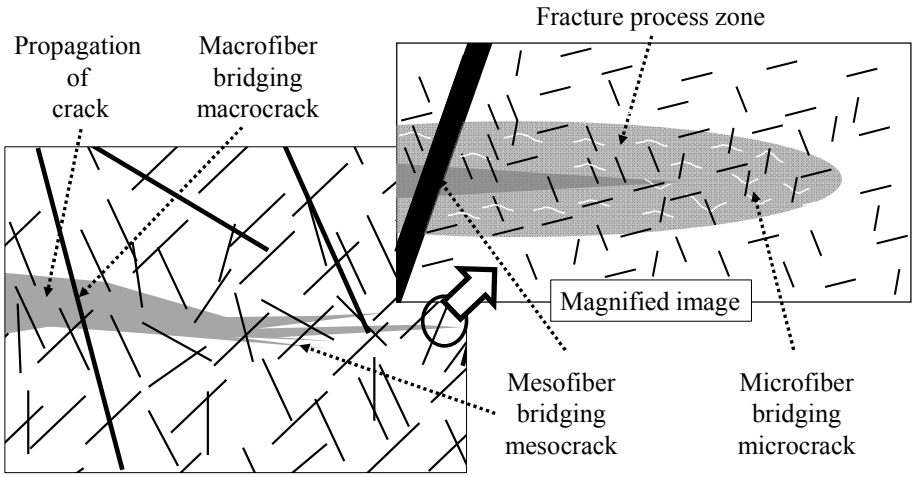

Fig. 1 Schematic illustration of multi-scale fiber-reinforcement system.

Table 1 Mix proportions.

Series	W/B [wt.%]	SP/B [wt.%]	D/B [wt.%]	S/B [wt.%]	Wo/B [wt.%]	Replacement ratio Wo/S [wt.%]
Control	15	1.3	0.02	48	-	0
Wo-A-10		1.5		43.2	4.8	10
Wo-B-10						
Wo-C-10						
Wo-A-20				38.4	9.6	20
Wo-B-20						
Wo-C-20						
Wo-A-27		1.8		35	13	27
Wo-B-27						
Wo-C-27		2.1				

Note: W: water, B: binder, SP: polycarboxylate-based superplasticizer,
D: anti-foaming agents, S: sand, Wo: wollastonite microfiber

Table 2 Properties of the wollastonite microfiber used in this study*.

Wollastonite type	Length [μm]	Diameter [μm]	Aspect ratio	Tensile strength [MPa]	Young's modulus [GPa]
Wo-A	50-2000	-	3-20	2700-4100	303-530
Wo-B	600	40	15		
Wo-C	156	12	13		

*Catalog values

materials show large deformation before fracture. The lack of ductility is often termed as brittleness.

3. Reinforcement effects of microfiber on the improvement of toughness of UHSM (Test I)

Experimental tests were carried out to investigate effectiveness of wollastonite microfiber to improve toughness of UHSM. The toughness of UHSM was evaluated by three-point bending tests on notched mortar beams. This type of test was selected to avoid brittle fracture of the UHSM. Authors conducted preliminary uniaxial tension tests on UHSM to investigate the effectiveness of wollastonite microfibers in improving the ductility by wollastonite as the microfiber. However, FRCC containing only wollastonite microfibers as reinforcement was found to exhibit very brittle failure irrespectively of the type and volume contents of the fibers. Thus, it was obvious that the uniaxial tension test is not suited to studying the effectiveness of wollastonite microfibers in improving the toughness of UHSM because of the very brittle behavior under uniaxial tension.

The influence of various types of wollastonite microfibers at various fractions on the toughness improvement of UHSM was investigated. Scanning electron microscope (SEM) was used to investigate toughening mechanisms of wollastonite microfiber by observing fracture surface of UHSM reinforced with wollastonite microfiber.

3.1 Materials, test setup, and procedure

The mix proportions of the microfiber-reinforced UHSM tested are shown in **Table 1**. The details of the mix proportions used in Test I are as follows. Commercial silica fume cement was used as a binder (B), with low-heat cement and silica fume premixed at mass contents of 0.82 and 0.18, respectively. The density and Blaine fineness of the B were 3.01 g/cm^3 and 6,555 cm^2/g, respectively. Well-graded, very fine natural silica sand (S) with an average particle size of 0.212 mm was used in this study. Wollastonite microfibers (Wo) ($CaSiO_3$) were used to reinforce the mortar. Three different sizes of Wo, shown in **Fig. 2** and **Table 2**, were used. The Wo-A fibers (hereinafter: Wo-A) varied relatively widely in length, from 50 and 2,000 μm. In addition, Wo-A varied more in length and diameter than the Wo-B fibers (hereinafter: Wo-B) and Wo-C fibers (hereinafter: Wo-C), as shown in **Fig. 2**. The aspect ratios of Wo-A, Wo-B, and Wo-C were almost the same, as shown in **Table 2**. The sand was partially replaced by wollastonite microfibers at weight contents (hereafter the sand substitution is called "re-

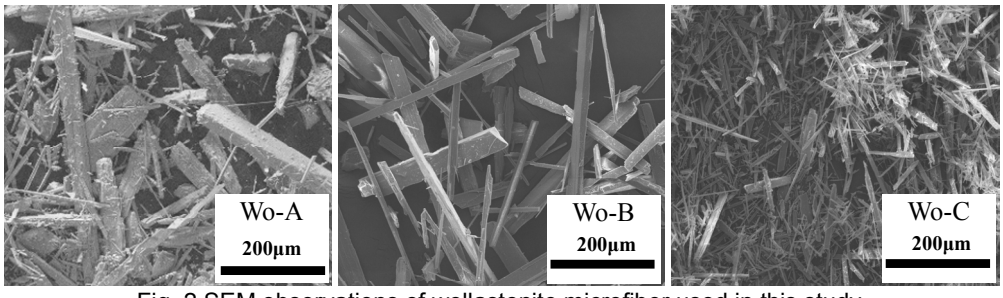

Fig. 2 SEM observations of wollastonite microfiber used in this study.

placement ratio") of 0%, 10%, 20%, and 27%. The highest replacement ratio (i.e. 27%) was selected on the basis of the results of preliminary mixing test on mortar to investigate the maximum weight contents of wollastonite microfiber. The respective densities of S and Wo were 2.6 g/cm^3 and 2.9 g/cm^3. A polycarboxylate-based superplasticizer (SP) and anti-foaming agents (D) were used to reduce the water dosage and air contents, respectively. An omni-type laboratory mixer with a capacity of 5 liters was used for mixing. The mixing procedure was as follows: (1) B, S, and Wo were dry-mixed for 1 min. (2) Water (W), pre-mixed with SP and D, was then added, and this mortar was mixed for 3 min.

Three-point bending tests on notched beams of UHSM were conducted for each series, according to the JCI recommendation (JCI 2003). Prism specimens were cast in steel molds of 40 × 40 × 160 mm^3 in size, as shown in **Fig. 3**. The specimens were cured in a moist curing room (temperature: 20 ºC, relative humidity: more than 95%) for 1 day. After unmolding, the specimens were cured in a steam chamber for 24 h. The steam curing conditions were as follows: the temperature was increased at a rate of 15ºC per hour up to 90ºC and then held at 90ºC for 24 h. The temperature was then gradually lowered to 20ºC. After steam curing, the specimens were stored in a curing room until the day of the testing. A notch of 20 mm deep was made at the center of each beam by means of a diamond cutter. The loading speed of the three-point bending tests was 0.01 mm/min and was controlled by displacement. The load and the crack mouth opening displacement (CMOD) were measured by means of a load cell and a clip gauge, respectively.

The fracture surfaces of specimen were observed by a scanning electron microscope (SEM) (JEOL JSM-6500F). The experimental conditions of magnification were 300x, 500x, 600x, 850x and 1000x. In addition, accelerating voltage was 15 kV.

3.2 Bridging mechanism of wollastonite microfibers and toughness index of UHSM

A schematic illustration of crack propagation in wollastonite-microfiber-reinforced UHSM is shown in **Fig. 4**. It is inferred that the wollastonite microfibers control crack initiation and propagation at the microscopic scale via bridging behavior, consisting of fiber rupture and pullout as well as crack deflection.

In order to evaluate the toughness of the mortar, toughness index was taken to be the area under the load-CMOD curve as an equivalent parameter to the work of fracture. To examine the toughness index of the mortar from the perspective of micromechanics, the area was subdivided into three regions, as shown in **Fig. 5**. In the first region, i.e., the elastic region, both the load and CMOD increase linearly up to the crack initiation load (P_{fcs}). The method used to detect P_{fcs} is shown in the enlarged view in **Fig. 5**. In the second region, strain hardening behavior is observed. Strain hardening can be caused by the bridging behavior of the aggregates and the wollastonite microfibers. In the third region, beyond the maximum load (P_{max}), cracks may propagate, and strain softening behavior was observed. In this region, the bridging, rupture, and/or pullout of the wollastonite

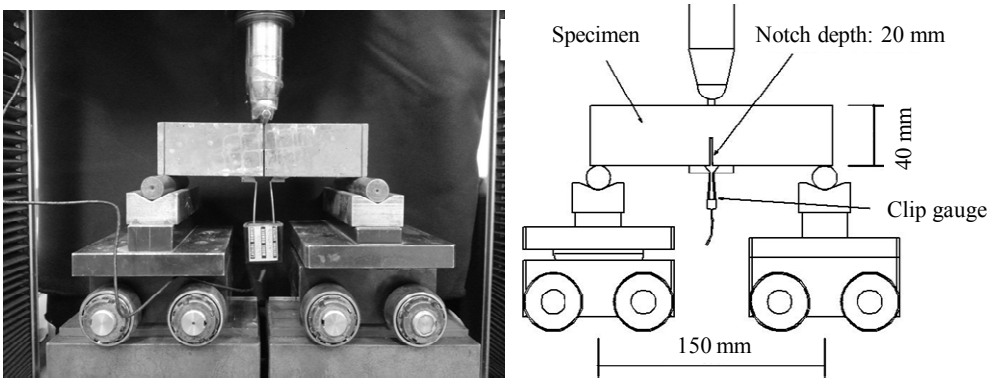

Fig. 3 Three-point bending test on notched beam.

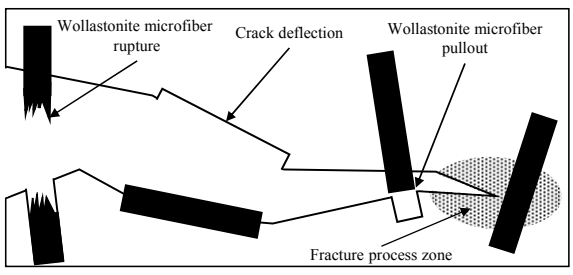

Fig. 4 Schematic illustration of crack propagation in wollastonite microfiber-reinforced UHSM.

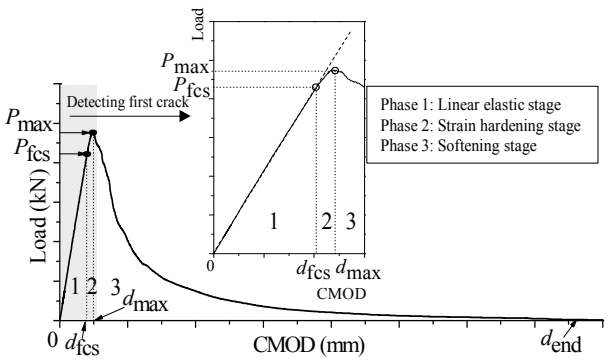

Fig. 5 Load-CMOD curve (one example of Wo series).

microfibers are expected to have a reinforcing effect. The gradual increase in the work of fracture that accompanies a nonlinear load-CMOD relation is correlated to the accumulation of internal cracking and the fiber bridging. Therefore, the reinforcing performance of the microfibers might be expressed by the work of fracture. To quantify the toughness index of the mortar in relation to the reinforcing mechanism, the following four parameters were defined:

$$W_{1,2} = \int_0^{d_{ts}} P(d)\mathrm{d}d \quad (1)$$

$$W_2 = \int_{d_{fcs}}^{d_{ts}} P(d)\mathrm{d}d \quad (2)$$

$$W_3 = \int_{d_{ts}}^{d_{end}} P(d)\mathrm{d}d \quad (3)$$

$$W_{1,2,3} = \int_0^{d_{end}} P(d)\mathrm{d}d \quad (4)$$

where $W_{1,2}$ = the amount of work up to the maximum load, d_{ts} = CMOD at the maximum load, d_{fcs} = CMOD at initial cracking, W_2 = amount of work from d_{fcs} to d_{ts}, W_3 = amount of work beyond the maximum load, d_{end} = CMOD at the end of loading, and $W_{1,2,3}$ = amount of total work.

3.3 Experimental results and discussion

(1) Observation of fracture surface of UHSM

The toughening mechanisms were investigated by observing the fracture surfaces of specimens by means of a SEM. Examples of the observed fractured surfaces of wollastonite-microfiber-reinforced UHSM specimens are shown in **Figs. 6 (a)-(e)**. Rupture and pullout of wollastonite microfibers were confirmed in **Figs. 6 (a)** and **(b)**, respectively. Evidence of crack deflection by wollastonite microfibers is also confirmed in **Fig. 6 (c)**. In addition, it was observed that the cement matrix was attached to the fiber surfaces in **Figs. 6 (d)** and (**e**). Wollastonite microfibers and mortar bond together by a hydration reaction whereby liberated $Ca(OH)_2$ reacts with the SiO_2 in the wollastonite microfibers to form C-S-H (Ransinchung and Kumar 2010). This might be another important factor in increasing the tensile strength and the toughness by chemical bonding between the fibers and the cement matrix.

(2) Toughness

Three specimens were tested for each test series in this study. The load-CMOD relationships of mortar reinforced with wollastonite microfibers at various replacement ratios are shown in **Figs. 7 (a)-(c)**. Almost no variation of all test series was confirmed and the mean curves of each series were represented in **Fig. 7**. The peak load is confirmed to increase with the replacement ratio of wollastonite microfiber as shown in **Figs. 7 (a)-(c)**. The highest peak load was obtained when the replacement ratio of wollastointe microfibers was 20% as shown in **Fig.7 (b)**. It might be because microfibers can arrest the prorogation of microcracks and delay the onset of localized crack formation. On the other hand, the result in case of 27% of replacement ratio showed a lower peak load than that in case of 20% of replacement ratio though W_2 became larger and the postpeak behavior became gentler than the case of 20% as shown in **Fig.7 (c)**. This is because a large number (i.e. 27%) of microribers caused defects in the matrix due to entrapped air or overlapping of fibers. Therefore, the peak load was lower than that in case of the replacement ratio of 20%. However, network structure including defects in the matrix, was established due to high replacement ratio of wollastonite microfiber and the toughness was highly

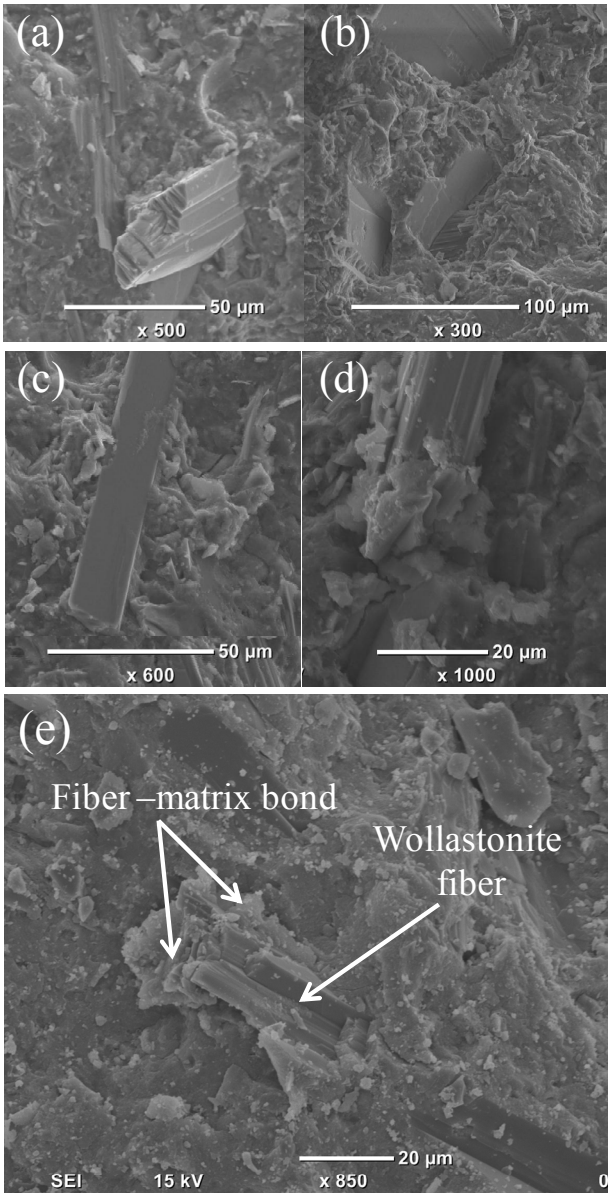

Fig. 6 SEM observations of flexural specimen fracture surfaces of wollastonite microfiber-reinforced UHSM: (a) rupture of wollastonite microfiber (b) pullout of wollastonite microfiber, (c) crack deflection, (d) and (e) fiber-matrix interfacial bond.

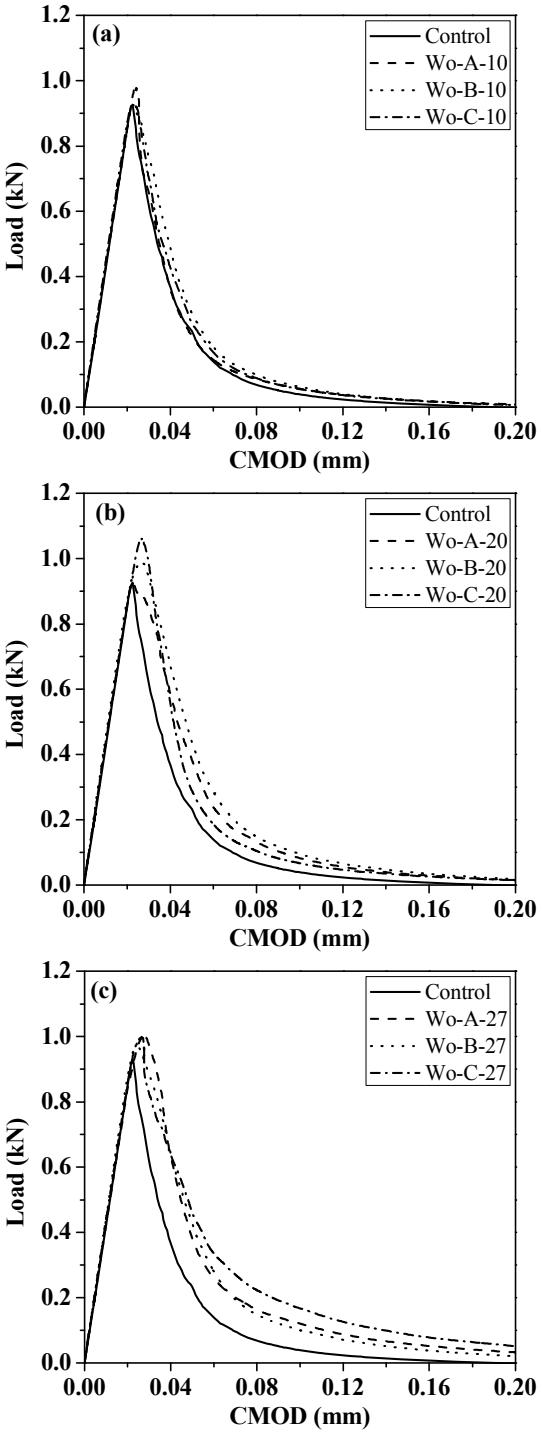

Fig. 7 Influence of wollastonite microfiber type and replacement ratio on load-CMOD curve.

increased by the mechanisms shown in **Fig. 4** after the first crack occurred in case of the replacement ratio of 27%.

The area under the load-CMOD curve was found to increase with the replacement ratio of wollastonite microfibers, at a rate that depends on the type of wollastonite microfiber. The toughness indices of each specimen were calculated from the load-CMOD curve, according to Eqs. (1)-(4). In order to assess the influence of the replacement ratio and type of wollastonite microfiber on the toughness indices, each toughness index value of the Wo series was divided by the corresponding value of the Control series which did not contain wollastonite microfiber. The obtained values were called as the normalized toughness index. The effects of wollastonite microfiber type and contents on the normalized toughness indices are illustrated in **Figs. 8 (a)-(d)**. Since all of normalized toughness indices had almost no variations, only the mean values are plotted. All of the Wo series exhibited higher values of normalized toughness index than those of the Control series.

Only the normalized toughness index W'_2 among four indices was found to proportionally increase as the replacement ratio of wollastonite microfiber increased. The wollastonite microfiber replacement ratio of 27% yielded the highest values for all four of the normalized toughness indices, in the order of Wo-C > Wo-B > Wo-A, except for $W_{1,2}$. Considerably higher values were observed for the W'_2 than for the other normalized toughness indices. This may be because the reinforcing effect of wollastonite microfiber is the strongest in the second region (W_2) shown in **Fig. 5**, during the strain hardening process after microcrack initiation.

The rate of increase is strongly dependent on the replacement ratio and the type of wollastonite microfiber. Among the three Wo series, the Wo-B and Wo-C series exhibited higher toughness than the Wo-A series. The Wo-A series contained microfibers of various aspect ratios, including relatively low ones (e.g., approximately 3), which are not sufficient to control cracking in the ways shown in **Fig. 4.** The Wo-C series exhibited higher toughness index values than the other series, which might be because the microfibers used in the Wo-C series have about the same aspect ratio as those used in the Wo-B series but are about a quarter of the length. As a result, the Wo-C series has a much larger total number of wollastonite microfibers per unit volume than the other series. Therefore, the Wo-C series might contribute more to bridging performance than the Wo-B. Another reason for the higher toughness index values of the Wo-C series is that the microfibers used in this series have a larger surface area than those used in the Wo-B series. Thus, in the Wo-C series, the chemical bond mechanism at the interface between the microfiber and the matrix shown in **Figs. 6 (d)** and **(e)** might work better than in the Wo-B series. Because of the reasons described above, even if the aspect ratios and mechanical properties of the wollastonite microfibers are approximately the same, thinner wollastonite microfibers can be more effective in increasing the toughness of UHSM than thicker ones.

4. Effect of microfibers on multi-scale fiber reinforcement (Test II)

Properties of hybrid fiber reinforced cement composites (HFRCC) was studied by Kawamata *et al*. (2003). They confirmed a plain matrix cannot sufficiently draw out

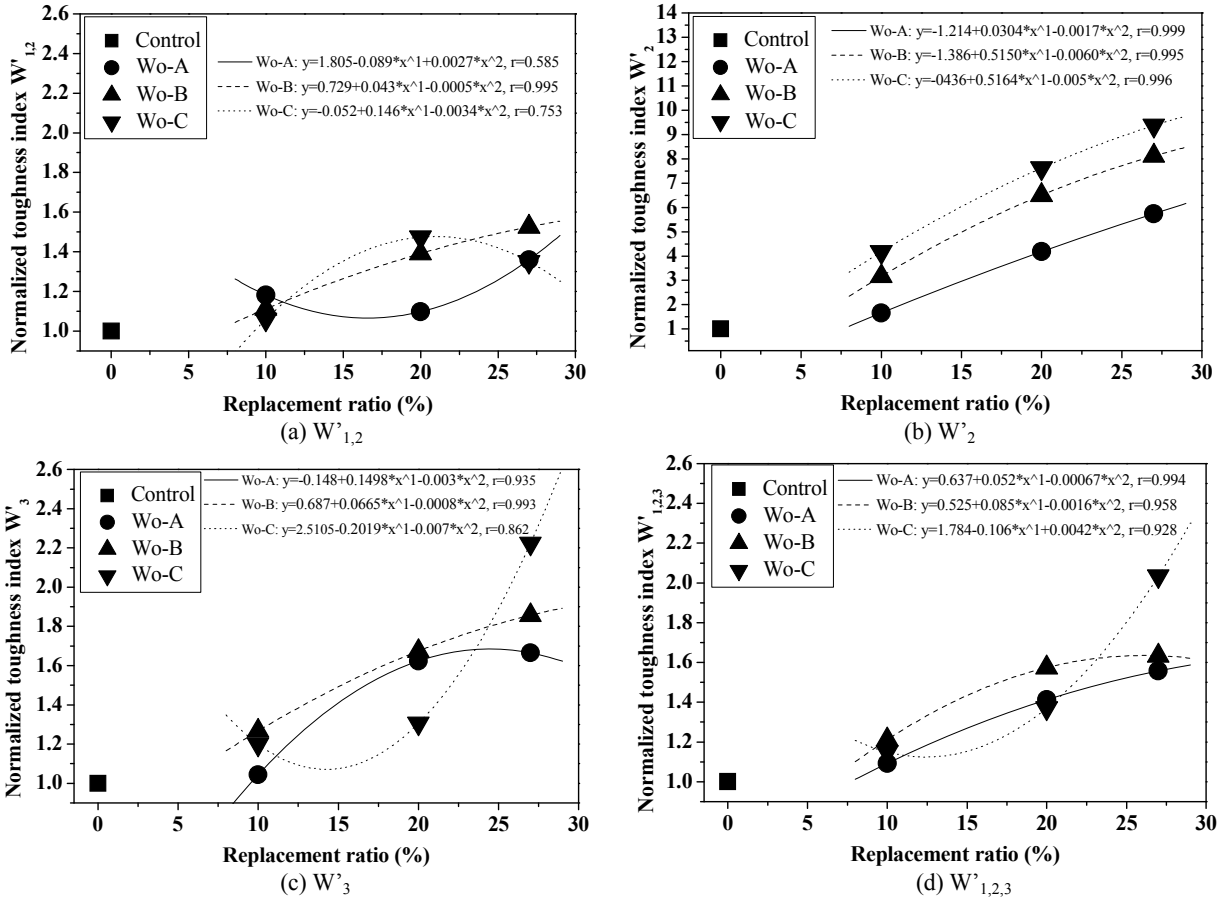

Fig. 8 Influence of wollastonite microfiber replacement ratio on normalized toughness index of each area.

the performance of macrofiber because of the coarse and wide cracks. Therefore, mesofiber (in the original paper, it was called "microfiber") was introduced. As a result, the ductility of the matrix was much improved and thinner multiple cracks were created around the notch tip. Hence, HFRCC showed higher performance of strength and toughness than those of FRCC. After Kawamata *et al*. (2003), Mihashi and Kohno (2007) explained the toughening mechanism of HFRCC by means of a series of pullout test on a single steel fiber by changing the inclination angle and the matrix. From the results, it is obvious that the most dominant factors for the absorbed energy among the given conditions are the type of steel fiber (i.e. bond due to snubbing) and the toughness of matrix. In other words, higher toughness of matrix increases the energy absorption capacity during the pullout process of steel fibers.

Then authors carried out a parametric study on the effects of the combination of meso- and macrofibers on the mechanical properties of UHP-FRCC (Kwon et al. 2013; Kwon et al. 2014). The studies clearly showed that increasing neither the total volume contents of fiber nor the volume contents of meso- or macrofiber do always increase mechanical properties of UHP-FRCC under tension because too tight distance (i.e. high volume contents of fiber) between meso- or macrofiber creates a kind of material defects. In addition, it was also clarified that tensile stress-strain curves of UHP-FRCC were dominantly dependent on the volume contents of macrofiber rather than that of mesofiber. Finally it was found that the best combination of volume contents of meso- and macrofibers were V_{meso} = 1.0% and V_{macro} = 1.5% as the minimum requirement for getting the ductile mechanical properties of UHP-FRCC in the previous studies.

However, influence of microfiber (i.e. wollastonite) on the mechanical properties of UHP-FRCC was not studied in the previous studies. Therefore, a parametric study of the influence of wollastonite on the mechanical properties of UHP-FRCC was experimentally carried out in this section based on the results of previous studies.

In Test II shown in this section, for confirming potential of wollastonite microfiber to increase mechanical properties of a multi-scale fiber-reinforcement system, influence of combinations of macrofibers, mesofibers, and different types of wollastonite microfibers was investigated. Three different types of wollastonite microfiber were used in this section and mechanical properties were evaluated by uniaxial tension test. This test could directly show tensile stress-tensile strain relationships. From the test results, tensile strength, tensile strain capacity and energy absorption capacity were discussed.

Table 3 Mix proportions.

Series	W/B [wt.%]	SP/B [wt.%]	D/B [wt.%]	S/B [wt.%]	Wo/B [wt.%]	Replacement ratio Wo/S [wt.%]	Mesofiber (vol.%)	Macrofiber (vol.%)
FRCC	15	1.3	0.02	48	-	-	1	1.5
FRCC-A-27		1.8		35	13	27		
FRCC-B-27								
FRCC-C-27		2.1						

Note: W: water, B: binder, SP: polycarboxylate-based superplasticizer, D: anti-foaming agents,
S: sand, Wo: wollastonite microfiber

Table 4 Properties of the fibers used in this study*.

Fiber type	Geometry	Specific gravity [g/cm³]	Length [mm]	Diameter [μm]	Aspect ratio	Tensile strength [MPa]
Mesofiber	Straight	7.85	6	160	37.5	2000
Macrofiber	Hooked	7.85	30	380	78.9	3000

*Catalog values

4.1 Materials, test setup, and procedure

In this study, employed materials and their mix proportion, mixing and curing methods were based on the authors' previous studies (Kwon et al. 2013, 2014). The mix proportions of the composite are shown in **Table 3**. The constituents of the UHSM were the same as those used in the Test I series that exhibited the highest toughness (i.e. replacement ratio: 27%). The volume contents of the meso- and macrofibers were V_{meso} = 1.0% and V_{macro} = 1.5%, respectively. Mesofibers used in this study were straight steel fibers with lengths of 6 mm and macrofibers were long and hooked steel fibers with a length of 30 mm. The diameter of the mesofiber was 0.16 mm, and that of the macrofiber was 0.38 mm. The density of steel fibers was 7.85 g/cm^3. The mechanical properties of the fibers are shown in **Table 4**. The mix proportions were developed by optimizing the parameters of several constituent materials. The mix had a compressive strength of 176-192 MPa. An omni-type laboratory mixer with a capacity of 5 liters was used for mixing. The mixing procedure was as follows: (1) B, S, and Wo were dry-mixed for 1 min.; (2) Water (W), pre-mixed with the SP and D, was then added, and this mortar was mixed for 3 min.; (3) The mesofibers were dispersed in the mortar mixture, which was then mixed for another 1 min and 30 s.; (4) Finally, the macrofibers were added, and mixing was resumed for another 3 min and 30 s.

Filling method of UHP-FRCC was fixed in the same way for each series, by keeping the pouring position of three parts to make two layers in the mould. Zhou and Uchida (2013) reported that fiber orientation was not changed if the placing method was same even though different length of fibers was used. Based on their experimental findings, the influence of the fiber orientation on mechanical performance was not discussed in the present study. Dog-bone specimens were cast in plastic moulds. The geometry of the dog-bone specimens is shown in **Fig.9**, which followed the recommendations of the Japan Society of Civil Engineers, (JSCE 2008) for High-Performance Fiber-Reinforced Cement-based Composites (HPFRCC).

The curing method was same as that for Test I. The equipment for mounting the dog bone specimens onto the loading machine and the setup for the uniaxial tension test are shown in **Fig. 9**. The average extension was measured over the central gauge length of 80 mm using two linear variable differential transducers (LVDTs)

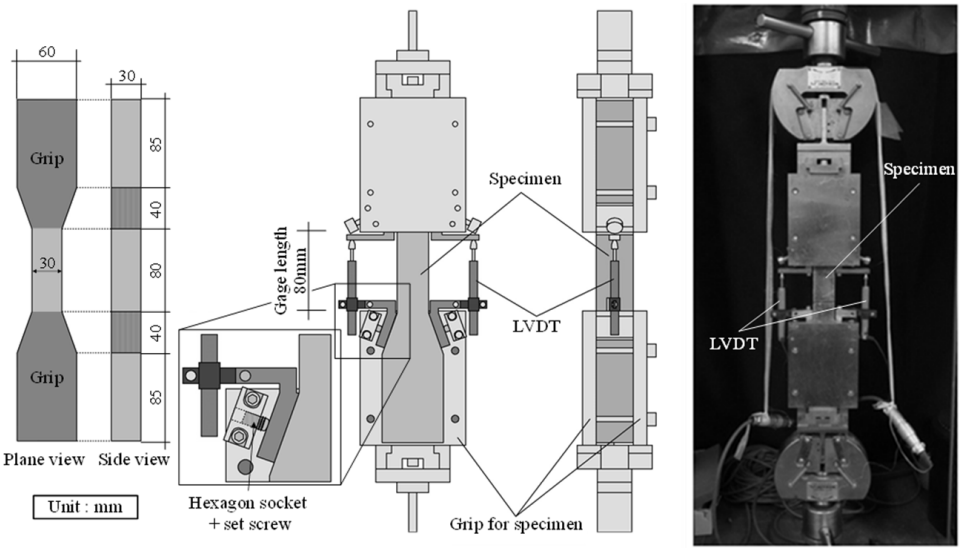

Fig. 9 Geometric properties of dog bone specimen and uniaxial tension test setup.

placed on both sides of the mounting frame and firmly clamped onto the specimen. A uniaxial tensile load was applied with a universal testing machine with 30-kN capacity. The support condition for the specimen was "fixed" at both ends. The tensile testing was conducted according to the recommendations of (JSCE 2008) for displacement-controlled uniaxial tension testing of dog bone specimens at a displacement rate of 0.5 mm/min.

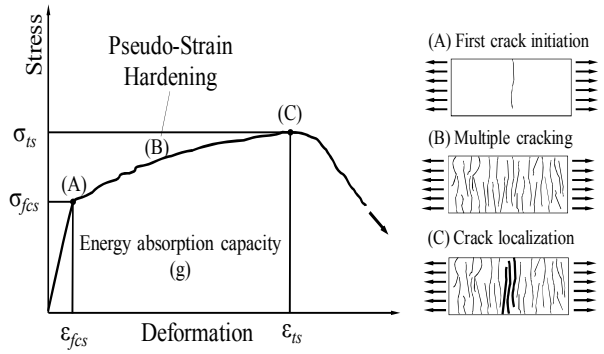

Fig. 10 Typical stress-strain relationships of HPFRCC. (after Naaman and Reinhardt 1996).

4.2 Strain hardening condition and tensile properties

The typical stress-strain relationship of HPFRCC under uniaxial tension is illustrated in **Fig. 10** (Naaman and Reinhardt 1996). Shape of the stress-strain relationship of UHP-FRCC is the same in principle as that of HPFRCC shown in **Fig.10**, though the strength of UHP-FRCC should be much higher than that of ordinary HPFRCC. The symbol σ_{fcs} represents the crack initiation stress, at which the first crack occurs, and σ_{ts} represents the tensile strength. The strain value at σ_{fcs} is the crack initiation strain (ε_{fcs}), and the strain at the tensile strength is defined as the strain capacity (ε_{ts}). Pseudo strain hardening means that the resisting tensile stress increases up to σ_{ts}, even after the first crack occurs at σ_{fcs}. According to Naaman and Reinhardt (1996), HPFRCC exhibit pseudo strain hardening with multiple cracks if the following condition is satisfied:

$$\sigma_{ts} \geq \sigma_{fcs} \tag{5}$$

The energy absorption capacity (g) of the UHP-FRCC was calculated by Eq. (6):

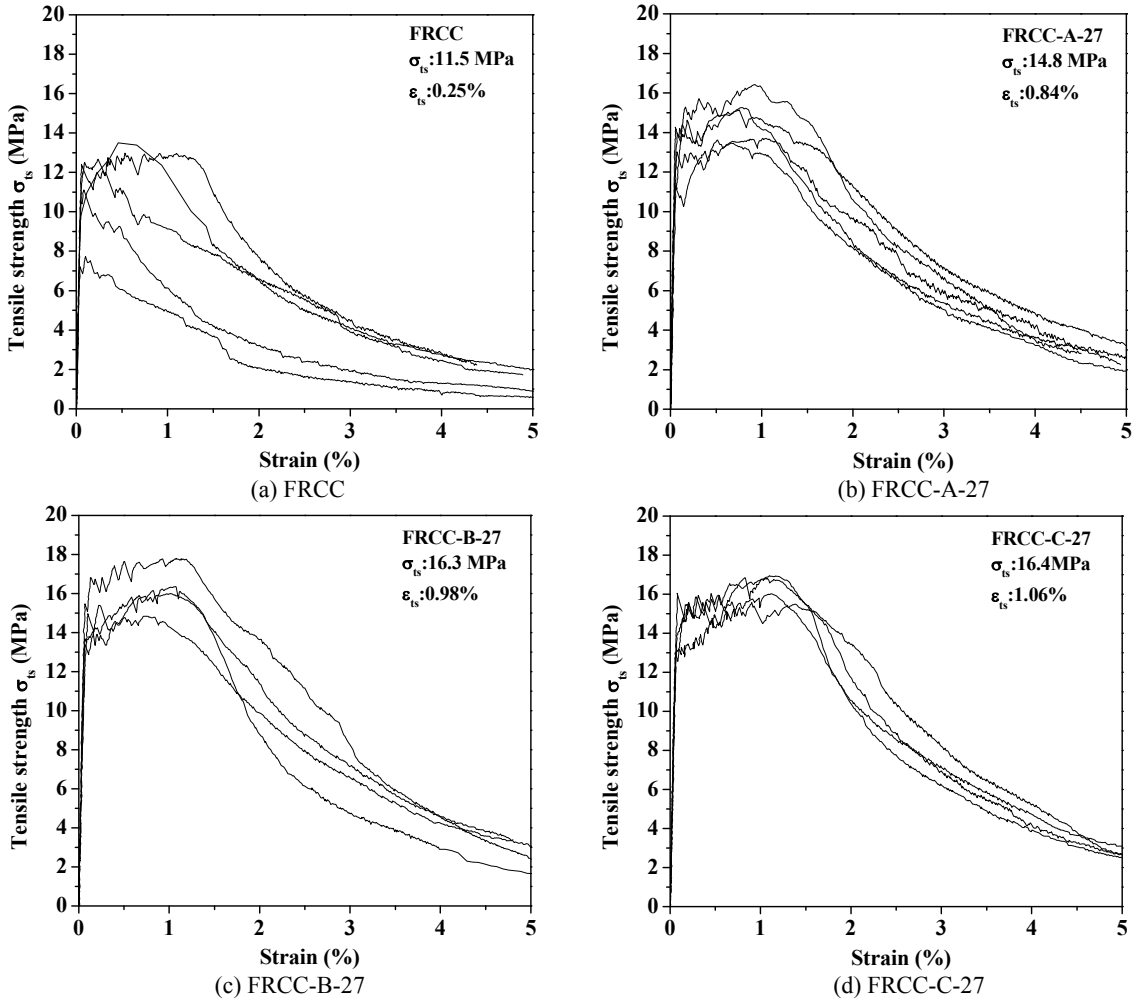

(a) FRCC (b) FRCC-A-27

(c) FRCC-B-27 (d) FRCC-C-27

Fig. 11 Tensile stress-strain curves of the UHP-FRCC specimens.

Table 5 Results of mechanical property tests.

Series	σ_{fcs} [MPa]	σ_{ts} [MPa]	ε_{ts} [%]	g [kJ/m^3]	Average number of cracks
FRCC	10.3	11.5	0.25	26	6
FRCC-A-27	12.8	14.8	0.84	112	11
FRCC-B-27	14.4	16.3	0.98	146	13
FRCC-C-27	14.0	16.4	1.06	156	14

Note: σ_{fcs}: average first crack strength, σ_{ts}: average tensile strength, ε_{ts}: average strain capacity, g: average energy absorption capacity.

$$g = \int_0^{\varepsilon_{ts}} \sigma(\varepsilon)\, d\varepsilon \quad (6)$$

which is equivalent to the area under the stress-strain curve from zero strain to ε_{ts}. The energy absorption during the strain softening phase is not discussed in this paper.

4.3 Experimental results and discussion

(1) Tensile stress-strain response of UHP-FRCC

The tensile stress-strain curves of all the specimens are illustrated in **Figs. 11 (a)-(d)**. All of the series exhibit strain hardening behavior. Large variations in the stress-strain curves are observed in the FRCC series, as shown in **Fig. 11 (a)**. The variations of the stress-strain curves in the FRCC-A-27, FRCC-B-27 and FRCC-C-27 series are considerably small in comparison with that in FRCC series, as shown in **Figs. 11**. In addition, the FRCC-A-27, FRCC-B-27 and FRCC-C-27 series exhibited higher tensile strength and strain capacity than those of the FRCC series, as shown in **Fig. 11**.

(2) Multiple cracking behavior and mechanical properties of UHP-FRCC

Multiple cracking was confirmed in all series. The number of cracks is directly related to the values of ε_{ts} and g, as shown in **Table 5**. The tensile strength, strain capacity, and energy absorption capacity are shown in **Figs. 12 (a)-(d)**. The mechanical properties of the UHP-FRCC decrease in the order of FRCC-C-27 >

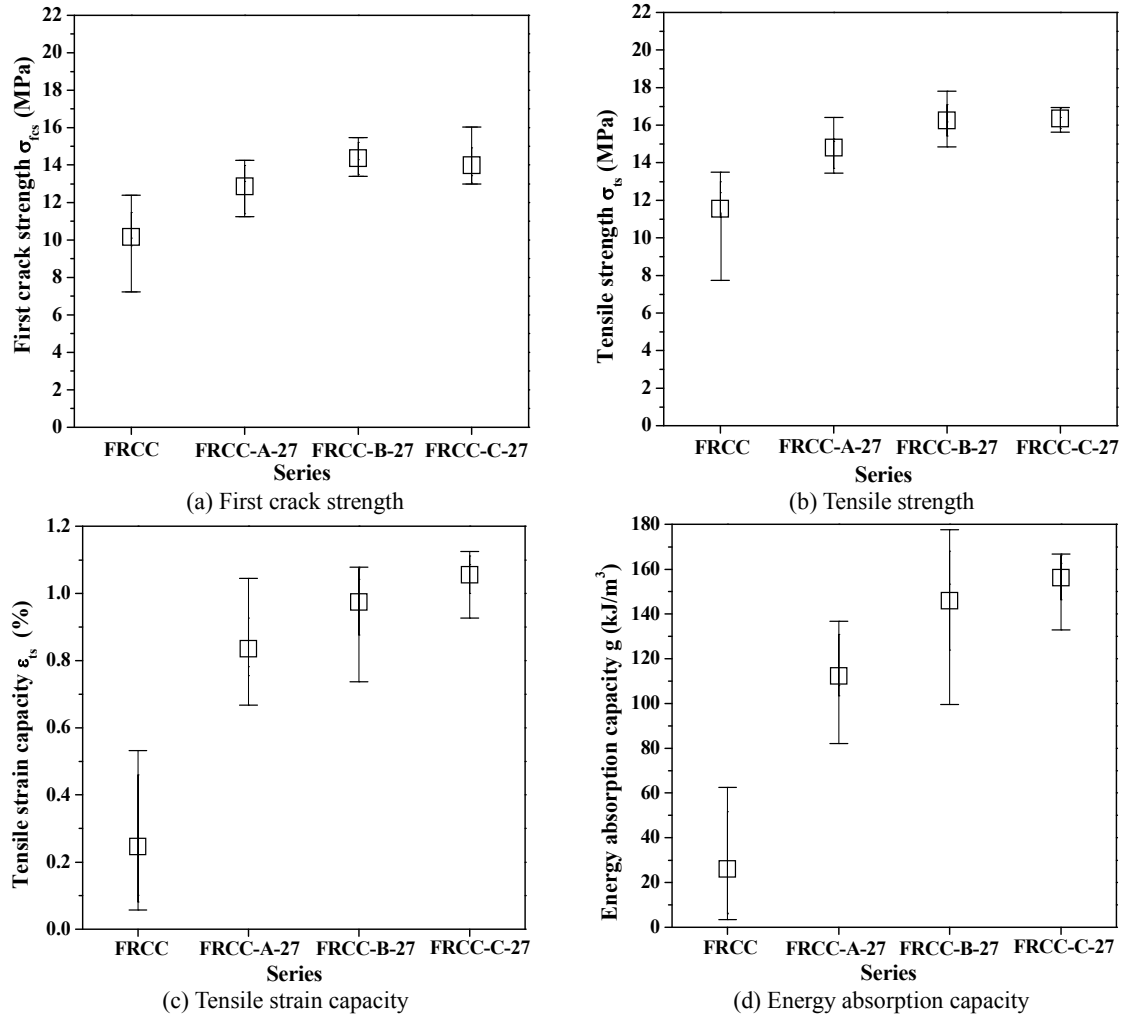

(a) First crack strength (b) Tensile strength

(c) Tensile strain capacity (d) Energy absorption capacity

Fig. 12 Comparison of first crack strength, tensile strength, strain capacity, and energy absorption capacity.

FRCC-B-27 > FRCC-A-27 > FRCC. Among the FRCC-A-27, FRCC-B-27 and FRCC-C-27 series, the FRCC-A-27 series exhibited the lowest values of the mechanical properties of interest, including σ_{fcs}, σ_{ts}, ε_{ts}, and g. This could be explained by the fact that the FRCC-A-27 series contains microfibers of relatively low aspect ratios which are not sufficient to control cracking in the ways shown in **Fig. 4**. The FRCC-C-27 series exhibited better mechanical properties than the FRCC-B-27 series. These results were consistent with those of Test I. FRCC-A-27, FRCC-B-27 and FRCC-C-27 series exhibited σ_{ts} values of approximately 15-16 MPa, which were higher than those of the FRCC series. The ε_{ts} and g values were approximately 3 to 4 times and approximately 4 to 6 times higher, respectively, than those of the FRCC series. In addition, among FRCC-A-27, FRCC-B-27 and FRCC-C-27 series, FRCC-C-27 showed the lowest scatter of mechanical properties as shown in **Fig.12**.

Relation between strain capacity (ε_{ts}) and energy absorption capacity (g) is shown in **Fig. 13**. Energy absorption capacity linearly increases as the strain capacity increases as shown in **Fig. 13**. It clearly shows the correlation between strain capacity and energy absorption capacity is very high. Consequently, it was confirmed in this study that the energy absorption capacity of UHP-FRCC was significantly influenced by the strain capacity.

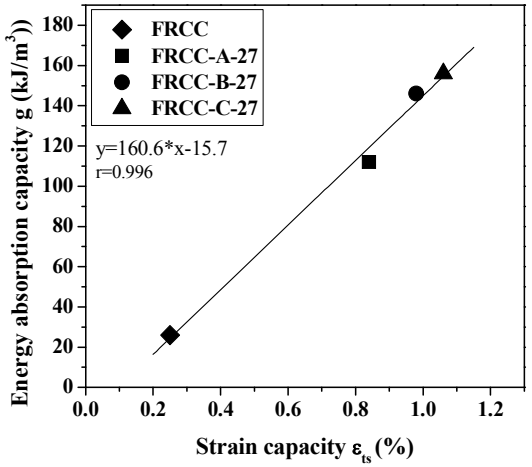

Fig. 13 Influence of strain capacity on energy absorption capacity.

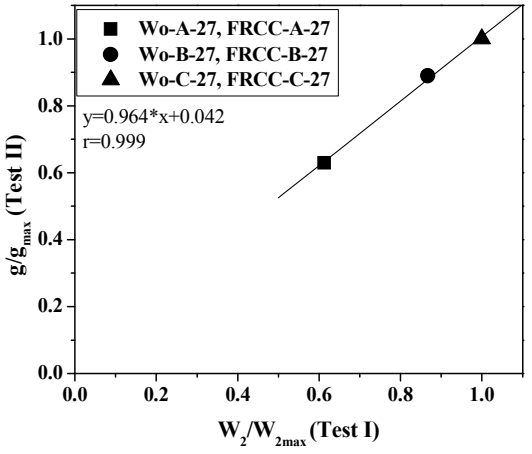

Fig. 14 Relationship between normalized toughness index W_2 (Test I) and normalized energy absorption capacity (Test II).

By comparing the results of Test I and Test II, it was suggested that toughness index of the matrix might have a dominant influence on the ductility of UHP-FRCC. Therefore, the authors investigated the correlation between the results of Test I and Test II. The relationships between the toughness index W_2/W_{2max} (Test I), and the energy absorption capacity (g/g_{max}) (Test II) are shown in **Fig. 14**, where both of them were normalized by the each maximum value. The results can be represented by a liner regression as a function of W_2 obtained in Test I, with a suitable correlation coefficient (r=0.999). Among the four toughness index parameters, W_2 was found to be the most highly correlated to g. Therefore, once the toughness of UHSM reinforced with wollastonite microfibers can be evaluated by means of three-point bending tests on notched mortar beams, the energy absorption capacity g of the UHP-FRCC could be estimated on the basis of the empirical formula obtained in this study. However, it is still reminded that the physical basis to estimate the energy absorption capacity of UHP-FRC from the toughness of UHSM should be discussed in the further study.

(3) Mechanism of multi-scale fiber-reinforcement system to increase ductility in UHP-FRCC

The obtained results described above proved that bridging microcracks by wollastonite microfibers is a very effective way to further improve the mechanical properties of UHP-FRCC. The possible mechanism to increase the ductility is discussed as follows: Since a large number of thin and short microfibers were dispersed densely in the matrix, propagation of microcracks is arrested to delay the crack initiation and propagation. Furthermore resistance of mesofibers against being pulled-out is increased by the additional bond stress caused by snubbing friction due to reinforcement of microfibers.

In addition, mesofibers also resist further crack opening in the mesoscale around the macrocracks (Kwon *et al*. 2014). Finally, macrofiber, which has high bond strength due to the geometry and a longer length, increases stress-transfer performance even after the meso- or macrocracks initiate. During the pullout process from the crack surface, macrofiber resists mechanically against crack opening in the macroscale because of the bending and yielding of the hooked part. Furthermore, because of the strengthened and stiffened matrix reinforced with the microfibers, friction of the macrofibers is also increased to enhance the bond property.

5. Conclusions

This study investigated the effectiveness of reinforcing

the matrix in the micro-scale with wollastonite microfibers to increase the ductility of UHP-FRCC. The following conclusions were drawn based on the obtained results.

1) The improvement in toughness of UHSM reinforced with wollastonite microfibers is highly dependent on the wollastonite microfiber contents (Test I). A particularly remarkable reinforcing effect was achieved in the strain hardening process that occurs after initial cracking.
2) In order to investigate the mechanism of toughness improvement achieved by wollastonite microfibers, the fracture surfaces of UHSM specimens were observed by means of SEM technique. Toughening mechanisms due to crack deflection at the micro-scale, rupture and/or pullout of wollastonite microfibers, as well as bond effect due to the chemical bond at the interface between the wollastonite microfibers and the matrix, were confirmed.
3) The results confirmed that the mechanical properties of UHP-FRCC, including tensile strength, strain capacity, and energy absorption capacity, increase dramatically as the replacement ratio of wollastonite microfibers increases (Test II). Moreover, the addition of wollastonite microfiber is effective in reducing the variation in stress-strain curves. Because of the above reasons, the multi-scale fiber-reinforcement system examined in this study worked well, and bridging microcracks by incorporating wollastonite microfibers was found to be very effective in improving the mechanical properties of UHP-FRCC.
4) Improvement in mechanical properties of UHP-FRCC reinforced with wollastonite microfibers was found to be dependent on the type of wollastonite microfibers used. For the purpose of improving the mechanical properties, it is desirable to avoid using the wollastonite microfibers of low aspect ratios. Moreover, among wollastonite microfibers with the same aspect ratio and mechanical properties, thinner wollastonite microfibers are more effective in increasing the mechanical properties of UHP-FRCC.
5) A strong correlation was found between the toughness index W_2 of UHSM and the energy absorption capacity g of UHP-FRCC. This may mean that bridging microcracks in the matrix by means of wollastonite microfibers might be a key to increase the energy absorption capacity of UHP-FRCC. However, it is still reminded that the physical basis to estimate the energy absorption capacity of UHP-FRC from the toughness of UHSM should be discussed in the further study.

Acknowledgements

The research described herein was partially sponsored by the Japan Society for the Promotion of Science under Grant No. 267167. The authors are grateful to the sponsor for its financial support. The authors are also grateful to Dr. F. U. A. Shaikh of Curtin University, Australia for his valuable comments.

References

Bache, N. H., (1992). "Principles of similitude in design of reinforced brittle matrix composites." In: H. W. Reinhardt and A. E. Naaman, Eds. *High performance fiber reinforced cement composites*, E&FN Spon. London, 39-56.

Boulay, C., Rossi, P. and Tailhan, J-L., (2004). "Uniaxial tensile test on a new cement composite having a hardening behavior." *In*: M. Di Prisco, R. Felicetti and G.A. Plizzaried, Eds. *6th International RILEM symposium on fibre-reinforced concretes (BEFIB' 2004)*, RILEM, Varenna, Italy, 61-68.

Chanvillard, G. and Rigaud, S., (2003). "Complete characterisation of tensile properties of Ductal® UHPFRC according to the French recommendations." *In*: A. E. Naaman and H. W. Reinhardt, Eds. *International workshop on high performance fiber reinforced cement composites*, RILEM Publications SARL, 21 - 34.

JCI, (2003). "Method of test for load-displacement curve of fiber reinforced concrete by use of notched beam." Tokyo: Japan Concrete Institute.

JSCE, (2008). "Recommendations for design and construction of HPFRCC with multiple fine cracks." Japan Society of Civil Engineers, Tokyo.

Jungwirth, J., (2006). "Zum tragverhalten von zugbeanspruchten bauteilen aus ultra-hochleistungs-faserbeton." Thesis (PhD). EPFL.

Kawamata, A., Mihashi, H. and Fukuyama, H., (2003). "Properties of hybrid fiber reinforced cement-based composites." *Journal of Advanced Concrete Technology*, 1(3), 283-290.

Kwon, S., Nishiwaki, T., Kikuta, T. and Mihashi, H., (2013). "Mechanical properties of ultra-high-performance hybrid fibre-reinforced cement-based composites." *International symposium on ultra-high performance fibre-reinforced concrete (UHPFRC 2013),* RILEM- fib-AFGC, Marseille, France, 669-708.

Kwon, S., Nishiwaki, T., Kikuta, T. and Mihashi, H., (2014). "Development of ultra-high-performance hybrid fiber-reinforced cement-based composites." *ACI Materials Journal*, 111(3), 309-318.

Lankard, D. R., (1984). "Slurry infiltrated fiber concrete (SIFCON)." *Concrete International*, 12, 44-47.

Maeder, U. Lallement-Gamboa, I., Chaignon, J., and Lombard, J.-P., (2004). "Ceracem, a new high performance concrete: characterizations and applications." *In*: M. Schmidt, E. Fehling and C. Geisenhanslüke, Eds. *International symposium on ultra high performance concrete*, Kassel, Germany, 59-68.

Magureanu, C., Sosa, I., Negrutiu, C. and Heghes, B., (2012). "Mechanical properties and durability of ultra-high-performance concrete." *ACI Materials Journal*, 109(2), 177-184.

Mihashi, H. and Kohno, Y., (2007). "Toughening mechanism of hybrid fiber reinforced cement composites." *6th International conference on fracture mechanics of concrete and concrete structures*, Taylor & Francis, Catania, Italy.

Mihashi, H., Rokugo, K. and Kunieda, M., (2010). "*Cracking and fracture mechanics of concrete -modelling of phenomena and control-*." Tokyo, Gihodo. (in Japanese).

Naaman, A. E., (1992). "SIFCON: Tailored properties for structural performance." *In*: A. E. Naaman and H. W. Reinhardt, Eds. *High performance fiber reinforced cement composites,* RILEM, ACI, Stuttgart University and the University of Michigan, E&FN Spon, London, 18-38.

Naaman, A. E. and Reinhardt, H. W., (1996). "Characterization of high performance fiber reinforced cement composites." *In*: A.E. Naaman and H.W. Reinhardt, Eds. *High performance fiber reinforced cement composites-HPFRCC2*, E&FN Spon, England, 1-24.

Orange, G., Dugat, J. and Acker, P., (2000). "DUCTAL: New ultra high performance concrete, damage resistance and micromechanical analysis." *In*: P. Rossi and G. Chanvillard, Eds. *5th RILEM symposium on fibre-reinforced concretes (FRC) (BEFIB' 2000)*, RILEM, Lyon, France, 781-790.

Ranade, R., Li, V. C., Stults, M. D., Heard, W. F. and Rushing, T. S., (2013). "Composite properties of high-strength, high-ductility concrete." *ACI Materials Journal*, 110(4), 413-422.

Ransinchung, G. D. and Kumar, B., (2010). "Investigations on pastes and mortars of ordinary portland cement admixed with wollastonite and microsilica." *Journal of Materials in Civil Engineering,* 22(4), 305-313.

Rossi, P., Acker, P. and Malier, Y., (1987). "Effect of steel fibres at two different stages: material and the structure." *Materials and Structures*, 20, 436-439.

Soliman, A. M. and Nehdi, M. L., (2012). "Effect of natural wollastonite microfibers on early-age behavior of UHPC." *Journal of Materials in Civil Engineering*, 24(7), 816-824.

Sujiravorakul, C., (2002). "Development of high performance fiber reinforced cement composites using twisted polygonal steel Fibers." Thesis (PhD). University of Michigan.

Wille, K., Kim, D. J. and Naaman, A. E., (2011). "Strain-hardening UHP-FRC with low fiber contents." *Materials and Structures*, 44(3), 583-598.

Zhou, B. and Uchida, Y., (2013). "Fiber orientation in ultra high performance fiber reinforced concrete and Its visualization." *8th International conference on fracture mechanics of concrete and concrete structures*, Toledo, Spain, 228-235.